Journal of Hazardous Materials Advances 7 (2022) 100104

Contents lists available at ScienceDirect

Journal of Hazardous Materials Advances

journal homepage: www.elsevier.com/locate/hazadv

An early comparison of nano to microplastic mass in a remote catchment's atmospheric deposition

Steve Allen[a,c,d,*], Dušan Materić[b], Deonie Allen[c,d], Anna MacDonald[c], Rupert Holzinger[b], Gael Le Roux[d], Vernon R Phoenix[c]

[a] Department of Earth and Environmental Sciences, Dalhousie University, Halifax, Canada
[b] Utrecht University, Institute for Marine and Atmospheric research Utrecht (IMAU), Utrecht, The Netherlands
[c] Department of Civil and Environmental Engineering, University of Strathclyde, Glasgow, Scotland
[d] Laboratoire écologie fonctionnelle et environnement, Université de Toulouse, CNRS, Toulouse, France

ARTICLE INFO

Keywords:
Aerosol pollutants
Transport processes
Microplastics
Nanoplastics
TD-PTR-MS

ABSTRACT

The existence of nano sized plastic (NP) has been discussed heavily in recent years, however physical proof from environmental samples and direct comparisons to characterized microplastics is limited. Here we compare microplastic (MP) particles and counts (>10 μm) to NP particle (<0.45 μm) mass concentrations from deposition at a remote field site in the French Pyrenees (elevation 1425 m a.g.l.). Using Thermal Desorption – Proton Transfer Reaction – Mass Spectrometry (TD-PTR-MS) analysis, the data shows that NP is present in atmospheric deposition in quantities up to 2.0×10^5 nanograms m^{-2} day^{-1} (1.1×10^5 nanograms m^{-2} day^{-1} standard deviation), comparable to that of the >10μm microplastic (up to 1.1×10^5 nanograms m^{-2} day^{-1}, 2.7×10^4 nanograms m^{-2} day^{-1} standard deviation). This comparison indicates the quantity of NP and MP may be similar in this atmospheric deposition, however the estimated particle count for NP is understandably multiple orders of magnitude greater compared to MP. Backward trajectory modelling was used to consider the transport of these MP and NP particles. This highlighted the extended spatial influence of NP and its propensity to remain elevated over a 7-day period.

Introduction

The issues surrounding plastic pollution are currently receiving multidisciplinary attention, with its discovery in all environmental matrices and in some of the most remote locations (for example, the Arctic, Antarctic, Alps and Ecuadorian Andes) (Ambrosini et al., 2019; Bergmann et al., 2019; Cabrera et al., 2020; Kelly et al., 2020). While research has focused on finding, quantifying and assessing the environmental impact of microplastics (MP, 1 μm-5 mm plastic particles), there is a growing interest in nanoplastic occurrence in the environment.

Nanoplastics have been described as plastic particles smaller than 1 μm and also confusingly as particles smaller than 100 nm. The definition of nano has meaning when applied to materials below 100 nm if that material behaves differently to its larger counterparts (Joachim, 2005). This is the level at which many materials start to exhibit Brownian motion (Feynman, 1963) as it bounces off molecules it is in suspension with. As both diffuse and ballistic Brownian motion are known to occur in particles up to 2.5 μm (Silica) in air, the term nano encompasses the small particle sizes in this study (Li & Raizen, 2013). Whist it is acknowledged that 100 nm is a practical limit for the safety regulations of industry, among the plastic pollution research community several papers and research groups consider and describe sub-micron synthetic polymer material as nanoplastic (NP are particles <1 μm) (Frias & Nash, 2019; Gigault et al., 2021). This simpler definition being easier for policy makers and the general public to understand without having to further explain the definition. With this in mind, the definition of NP used in this study is 1 nm -1 μm.

Nanoplastic particles form an important element in the global plastic cycle and plastic pollution impact (Allen et al., 2022; Mitrano et al., 2021). NP occur as primary (designed as nano sized plastic particles) or secondary (larger particles degraded to nano size) and their presence has been inferred from assessment of marine waters (Gonçalves & Bebianno, 2021; Piccardo et al., 2020), soil (Wahl et al., 2021), air (Materić et al., 2021) and biota (Ferreira et al., 2019). NP can be more easily taken up (ingested, inhaled or adsorbed) by biota due their small size (Banerjee & Shelver, 2021), entering the ecosystem. Due to the small size and often jagged shape, secondary NP (and small MP) can pass through or impact on epithelial membranes and early studies suggest there may be a link between changed function, compromised immune systems and cytotoxicity (Deng et al., 2020; Huang et al., 2020; B. Li et al., 2020). As a result, NP could potentially influence the cellular to organism functionality, a concern to both environmental and human health

* Corresponding author.
E-mail address: st504087@dal.ca (S. Allen).

https://doi.org/10.1016/j.hazadv.2022.100104
Received 25 April 2022; Received in revised form 31 May 2022; Accepted 2 June 2022

(Banerjee & Shelver, 2021; Rubio et al., 2020; Wright & Kelly, 2017; Yee et al., 2021). Given this risk, understanding the extend of MP and NP pollution is crucial. The ratio of MP to NP is still generally hypothesised, with limited data to directly compare MP to NP within individual samples. Formative studies indicate notable atmospheric NP mass (in snow and dry atmospheric deposition) 42 (+32/-25) kg km^{-2} $year^{-1}$ (Materić et al., 2021) and 13.2-52.3 ng mL^{-1} (in ice) (Materić et al., 2022).

Nano sized plastics (NP, 1 nm -1 μm) have been difficult to assess in environmental matrices due to their small size. Published and functional limitations of individual particle spectroscopy are approximately μRaman-1 μm and FTIR-10 μm (Xu et al., 2019; Zheng et al., 2021). The limitations of environmental mass concentration analysis by methods such as Py-GCMS are micrograms (Akoueson et al., 2021; Okoffo et al., 2020). The vast majority of studies assessing NP have thus far have been theoretical or laboratory based, providing a limited understanding of the possible quantities in the environment. However, recent research from Materić et al. (Materić et al., 2020, 2021, 2022) illustrates the effective use of Thermal Desorption – Proton Transfer Reaction – Mass Spectrometry (TD-PTR-MS) for environmental NP analysis. The use of this new method has paved the way for analysis of the elusive nanoplastics in environmental samples.

Materials and methods

Atmospheric deposition samples were collected from the remote mountain location of Bernadouze, a long-term monitoring station in the central Pyrenees, France (42° 48′ 14.6″ N, 1° 25′ 06.8″ E, 1,425 m above mean sea level). Standard total atmospheric deposition collectors were used over the course of 5 months, November to March 2018, to collect monthly cumulative total deposition (sample time steps were constrained by access due to snow closure of the access road) (Sample durations: November – 12 days, December – 19 days, January – 34 days, February – 41 days, March – 34 days). Samples were collected as total atmospheric deposition (wet + dry deposition) using a Palmex Rain Sampler (sampling area of 0.014 m^2, open diameter of 135 mm) and a NILU Particle Fallout Collector (sampling area of 0.03 m^2, open diameter of 22 mm). Both samplers had sufficient capacity to ensure no overflow occurred during the sample period (in excess of 3 L). Atmospheric deposition collectors were open for the full sampling period and acted as duplicate sample sets. Multiple field blanks that underwent the full laboratory procedural process were collected on site during this sampling period (November – March 2018) (additional field blank information provided in Supplementary Information). Sample collectors were rinsed thoroughly on site (3 times, approximately 250 mL) with MilliQ water and the sample was decanted into sterilised glass containers (including the equivalent field blanks) and transported back to the laboratory where they were stored in a temperature controlled, dark, fridge (4 degrees) until sample preparation and analysis (Allen et al., 2019).

Samples were pre-filtered through a 0.45 μm pore 47 mm diameter polytetrafluoroethylene (PTFE) filters that had been pre-flushed using filtered MilliQ water (250 mL MilliQ flush) (Materić et al., 2020). The filtrate was placed in sterilised 25 mL glass vial for TD-PTR-MS analysis (vials prepared by heating to 450 °C overnight (in a Carbolite CWF1200 oven/kiln), sterilised containers were wrapped in sterilised aluminium foil after heading to minimise external contamination). No sample pretreatment was undertaken. The remaining material on the PTFE filter was then flushed with H_2O_2 (30% w/w) into covered, sterilised borosilicate glass test tubes in a dry heat block at 55 °C to complete organic digestion (7 d with no agitation, further peroxide added on day 8 if necessary and second 7 day digestion at controlled temperature completed) (Allen et al., 2019). After organic material was adequately removed the sample was filtered onto pre-flushed PTFE filters to remove residual H_2O_2 and liquid and then flushed into sterilised glass density separation tubes with $ZnCl_2$ (1.6 g mL^{-1} density) and agitated to aid MP separation from mineral and residual organic material (Allen et al., 2019). Due to the use of PTFE filters, PTFE particles and mass were not counted within this study. Settled material was removed from the bottom of the density separation tubes and the remaining upper liquid plus microplastic material was filtered onto 25 mm diameter aluminium oxide (Whatman Anodisc) filters for μRaman analysis.

The samples were analysed for MP by μRaman spectroscopy (785 nm laser, 1200 l/mm grating, scanning 200-2000 cm^{-1} with 15s acquisition time and 10 accumulations) and Nile Red fluorescence to quantitatively characterise the atmospheric deposition of MP at this site for this monitoring period (Allen et al., 2019). Raman spectra analysis was undertaken using open source Spectragryph software and available databases (Menges, 2018; Munno et al., 2020; Primpke et al., 2020). The limits of quantification for μRaman analysis for these samples was set to 10 μm.

NP analysis was completed as a blind test by Thermal Desorption – Proton Transfer Reaction – Mass Spectrometry followed protocols previously developed by Materić et al. (2020) herein briefly described. TD-PTR-MS is a destructive analytical method, similar to Py-GCMS, but can be used for nanoplastic analysis in line with microplastic assessment. Filtered (<0.45 μm) samples were well mixed (shaken but not vortexed to ensure sample particle integrity) to ensure homogeneity throughout the sample, then sub-sampled into three 0.5 mL replicates that were individually analysed by TD-PTR-MS (PTR-MS model PTR8000, IONICON Analitik, Austria) directly via sterilised glass vials (10 mL) (Materić et al., 2020). Field blanks were analysed in the same way and used to blank correct all results. Process blanks were carried out using MilliQ water and underwent the same procedures and durations as the samples and quantities subtracted from final results (see supplementary information). The TD-PTR-MS analysis of NP was undertaken using the fingerprinting algorithms created and published in Materić et al., 2020, 2021, 2022.

All samples and field blanks were transported to the laboratory where sample preparation occurred in a clean and access-controlled space. Field blanks underwent full procedural processing and analysis therefore representing the cumulative field activity and procedural activity contamination potential. Additional lab procedural blanks were created and analysed specifically for NP analysis and sample blank correction (see supplementary information). Cotton clothing and lab coats were worn to minimise sample contamination and laboratory surfaces were cleaned and covered with non-plastic material (sterilised aluminium foil). Field blanks were processed following the same procedures (full process blanks) (Allen et al., 2019) and counts subtracted from the final results (counts in supplementary).

Results and discussion

MP and NP quantitative characterisation

The μRaman analysed MP particle counts and polymer types and the TD-PTR-MS analysed NP mass and polymer types were compared by calculating the respective mass and particle counts for each sample (see Supplementary Information and data for additional details). MP results were converted from particle count to mass relative to their particle size following. The resulting mass were presented relative to particle size (Fig. 1c) and to total MP in each sample (>10 μm) (Fig. 1a). Similarly, the NP mass relative to polymer type (<0.45 μm) were converted to particle counts (assuming a spherical conservative particle size of 0.45 μm) to enable direct comparison to the MP particle counts (Fig. 1b, c). It is noted that some of the NP particles within the samples may have resulted from UV degradation during the more extended sample durations (e.g. samples over 34 to 41 days). However, analysis of the environmental MP stability to UV degradation over this sample period was beyond the scope of this study. The total deposited MP >10 μm mass ranged between 44×10^3 - 109×10^3 ng m^{-2} day^{-1} with an overall average for the monitoring period of 87×10^3 ng m^{-2} day^{-1}. Comparably, total NP <0.45 μm mass ranged from below detection to 203×10^3 ng m^{-2} day^{-1}, with an average NP mass for the monitoring period of 50×10^3

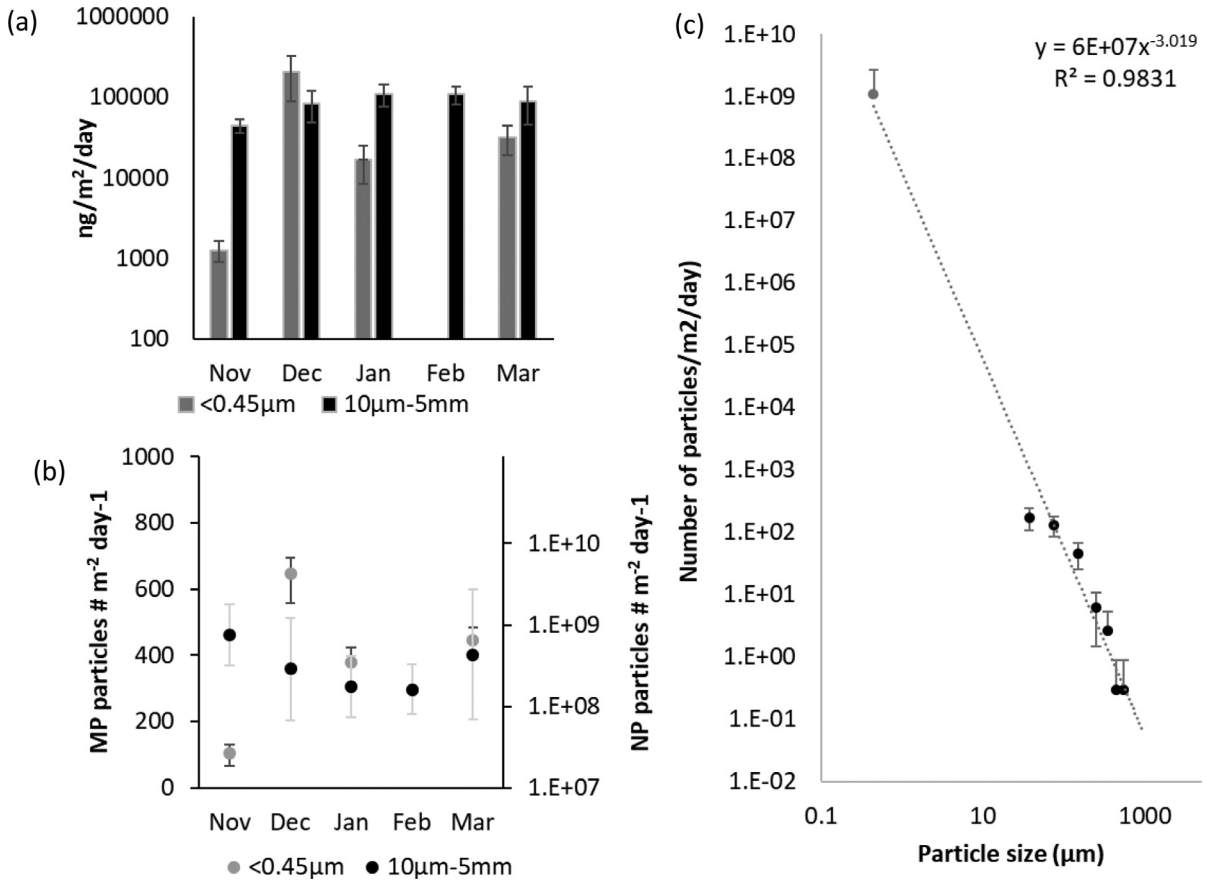

Fig. 1. Comparison of NP and MP mass (a), number (b), and the relative number of particles across samples considering both the analysed MP and NP results (c). It is noted that the NP results for February fell below the limits of quantification.

ng m^{-2} day^{-1}. The mass of MP >10 µm and NP <0.45 µm deposited at this location for this period is comparable (average results and range are within an order of magnitude) and are in agreement with the simulated NP fibre and MP release experiment findings of Yang et al. (2021). The NP mass results (18 (+55/-17) kg km^{-2} $year^{-1}$) are also comparable to previously published results, 42 (+32/-25) kg km^{-2} $year^{-1}$ (Materić et al., 2021).

Particle counts for MP >10 µm were several orders of magnitude lower than that calculated for NP <0.45 µm. MP and NP particle counts have been shown to increase with decreasing particle size (Kooi & Koelmans, 2019), resulting in up to orders of magnitude greater particle counts as macroplastic degrades to MP and NP. MP particle counts ranged from 297- 462 particles m^{-2} day^{1} (average of 365 particles m^{-2} day^{1}) whereas NP estimated particle counts (adopting the conservative particle size of 0.45 µm) ranged from below detection to 43×10^{8} particles m^{-2} day^{1} (11×10^{8} particles m^{-2} day^{1}). This agrees with the increasing particle count relative to decreased particle size found in both microplastic and nanoplastic studies (Bianco & Passananti, 2020). This suggests that while comparable mass of MP and NP occur in the atmospheric deposition at this site, a far greater number of NP particles are being deposited compared to MP.

To ensure comparability, five of the classic hydrocarbon based polymer types were specifically analysed (polystyrene-PS, polyethylene-PE, polypropylene-PP, polyvinyl chloride-PVC and polyethylene terephthalate-PET) (Plastics Europe & Organisations, 2021). Multiple plastic polymer types were found in each sample at both MP and NP particle size range (Fig. 2a). With the exception of the February NP sample where results were below detection limits, all samples contained PVC as both MP and NP. Similarly, PET was found in all NP samples (excl. Feb) but was absent in the MP samples for November and March. Conversely, PE and PP were found in the MP samples for January, but reported below the limits of detection for NP in the same samples.

The overall (cumulative) mass of each plastic type for MP and NP is comparative (Fig. 2b), with greater NP quantities of PVC, PET and PP compared to MP. When compared as a proportion of the total mass of MP or NP, this differentiation in polymer composition is more easily visualised, with PS, and PE predominantly occurring as MP, PP occurring in moderate proportions in both MP and NP particle size ranges, and PVC and PET occurring predominantly in NP.

There does not appear to be a direct link between MP and NP polymer type occurrence in this limited dataset, and it is suggested this may be because of the long-distance transport and distal source of MP and NP. The deposited MP and NP may have been transported an extensive distance (100's km) and due to their different particle characteristics may have come from different sources and travelled different distances due to the relative remote location of the sample collection site, and therefore may not be directly related.

MP and NP atmospheric transport

Simple, indicative atmospheric back trajectory and air/particle history modelling can provide a valuable insight into where MP and NP may have been transported from, what elevation in the atmosphere they were transported through, and how far they have travelled. To provide a high level comparative overview of MP and NP atmospheric transport for particles deposited at this Pyrenean field site, long time step atmospheric particle transport modelling was undertaken. This modelling was designed to illustrate the difference in atmospheric transport (extent, elevation) between MP and NP and not to be prescriptive or illustrative of individual sample findings in detail.

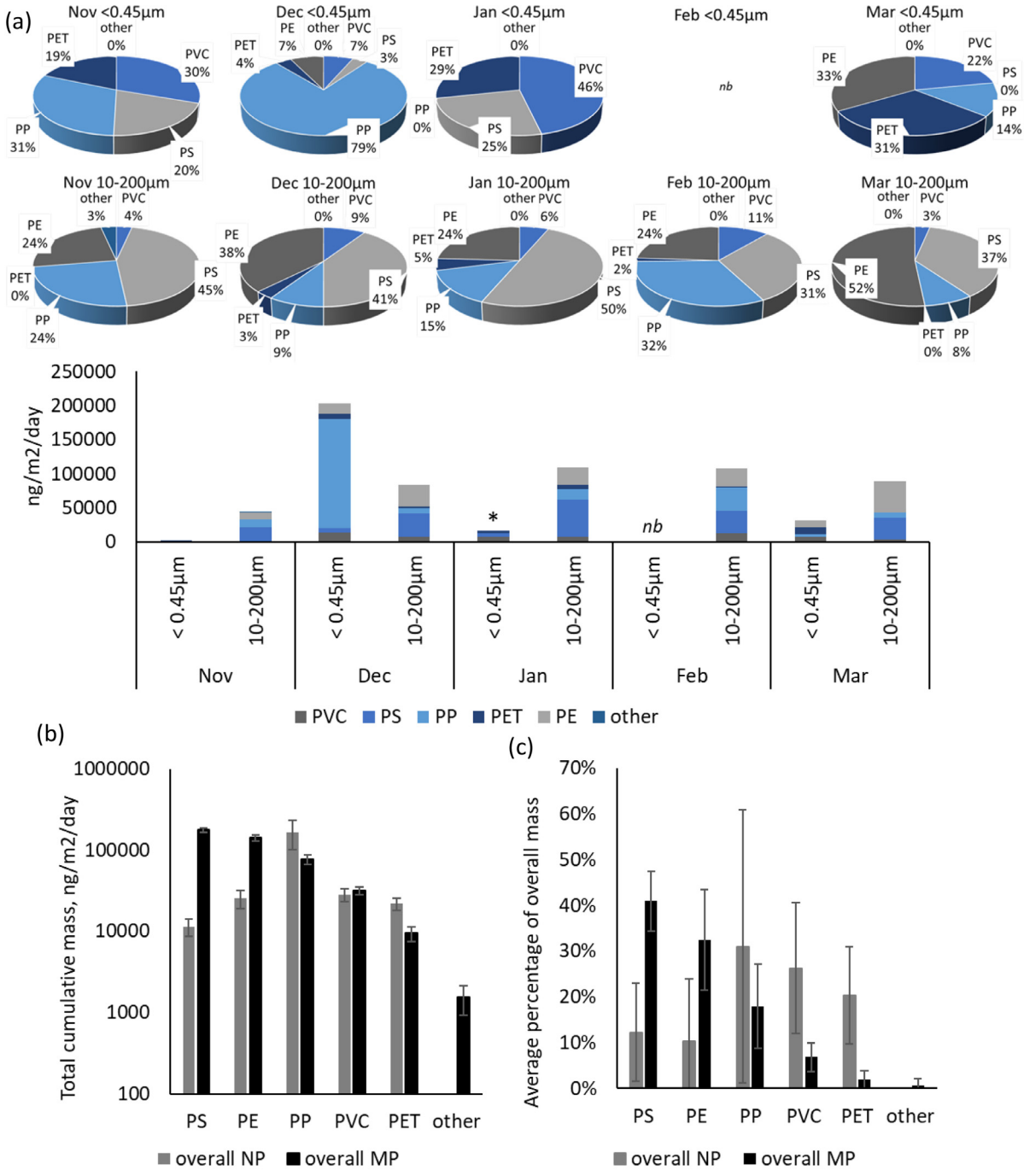

* denotes the <0.45µm mass of plastic in the January sample after the detection limit is lowered from 80% to 30% accuracy. At 80% both January and February present <0.45µm plastic masses below the detection limit (<10ng/ml). When the accuracy of plastic identification is loosened from an 80% correlation to a 30% correlation (of spectral peaks) then PP, PET and PVC can be identified and quantified in the <0.45µm samples for January. *nb* denotes the <0.45µm mass of plastic in the February sample that fall below the limit of quantification.

Fig. 2. Types of plastic found in the MP atmospheric deposition and NP deposition. Fig. 2(a) presents the mass of each polymer type within each sample relative to the two particle size groups (NP < 0.45 µm or MP < 10 µm), (b) the mass of each polymer type over the total monitoring period relative to the particle size (NP < 0.45 µm or MP < 10 µm), (c) the percentage of polymer relative to the total MP (or NP) mass. Further information is provided in the Supplementary information.

*denotes the <0.45 µm mass of plastic in the January sample after the detection limit is lowered from 80% to 30% accuracy. At 80% both January and February present <0.45 µm plastic masses below the detection limit (<10 ng/mL). When the accuracy of plastic identification is loosened from an 80% correlation to a 30% correlation (of spectral peaks) then PP, PET and PVC can be identified and quantified in the <0.45 µm samples for January. *nb* denotes the <0.45 µm mass of plastic in the February sample that fall below the limit of quantification.

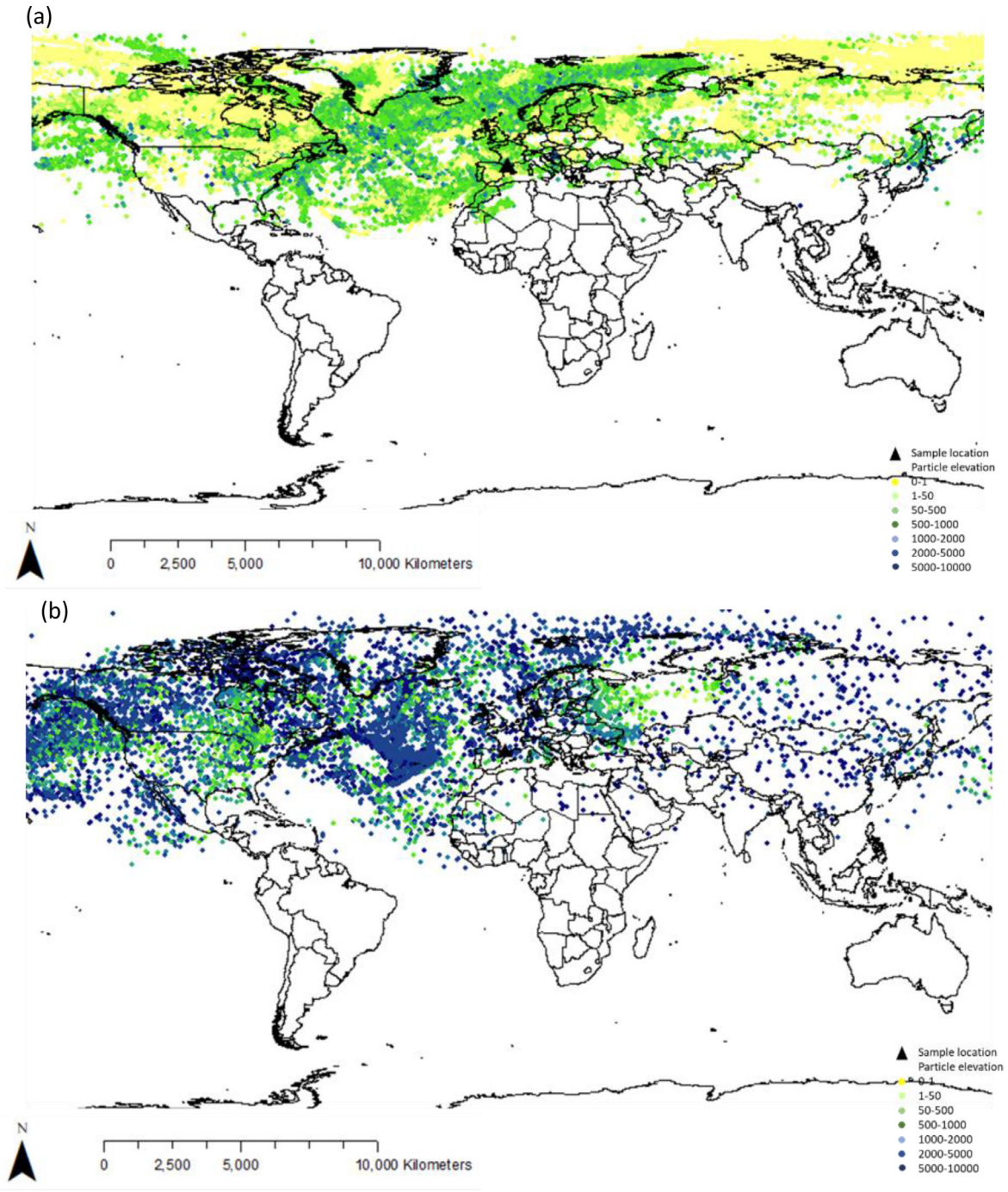

Fig. 3. MP (a) and NP (b) particle plot for all sample periods with the respective particle elevation above ground level.

Controlled environment laboratory examination of the field/laboratory assessed atmospheric settling velocity of MP or NP particles is a new area of research, but early atmospheric modelling has been completed using estimations of MP settling velocities from Stokes Law (Allen et al., 2019; Trainic et al., 2020; Wright et al., 2020). Therefore, for the purposes of this discussion, MP settling velocities have been calculated using Stokes Law, to consider the potential atmospheric transport of sampled MP and to compare this to the potential atmospheric transport of newly quantified NP. For simplicity, particles were considered to be cylindrical (acknowledging that fibres or a range of lengths and diameter were found in the MP samples and that NP particle shapes were not defined). For the purposes of this modelling assessment MP particles were defined as 25 μm (the predominant size range for the MP particles) and NP as 0.45 μm (acknowledging that there will potentially have been greater particle counts for smaller particle sizes in the NP samples). Settling velocities for the 25 μm and 0.45 μm generic plastic particles were calculated following:

$$V_t = \frac{g d^2 (\rho_p - \rho_m)}{18\mu}$$

Where g is acceleration due to gravity (9.8m s^{-2}), ρ_p defines the density of the plastic particle (1 g cm^{-3}), ρ_m is the density of the medium (air, 1.27 kg/m^3 at 5 °C), and μ is the dynamic viscosity of the medium (air, 1.74×10^{-5} kg m^{-1} s^{-1} at 5 °C). Settling velocities were estimated as 0.02 m/s for 25 μm MP spheres and 6.3×10^{-6} m s^{-1} for 0.45 μm plastic particles. This results in a simplistic atmospheric transport time (from

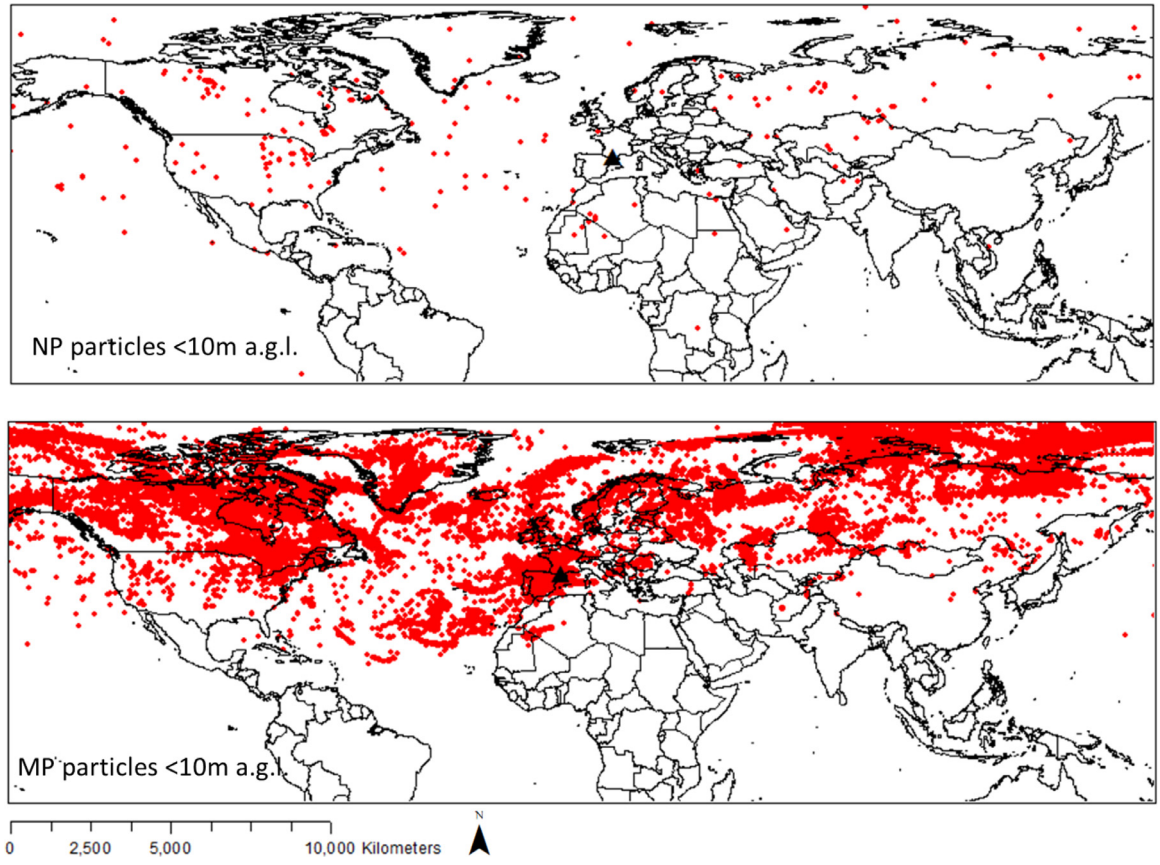

Fig. 4. Visualisation of particles at or below 10m a.g.l. during the backward trajectory particle modelling.

estimated planetary boundary layer upper elevation of 600 m Above Ground Level (a.g.l.)) of 8.5 hours for a 25 μm MP particle if no dynamic mixing, turbulence or change in atmospheric conditions occurred during transit. For the smaller particles, this duration extends out past one month (>744 hrs). The dynamic mixing, atmospheric characteristics, particle removal due to precipitation (scavenging) and dry deposition therefore potentially have a significant influence on the transport and deposition of these <0.45 μm particles.

To illustrate the potential influencing area of MP relative to NP, the dynamic HYSPLIT atmospheric transport modelling for the sample particles was completed relative to selected size and settling velocities. Whilst it is clear that the ~ 1 month time step for sampling precludes accurate particle back trajectory analysis for the specific samples, the following analysis was carried out to attempt to elucidate any difference between micro and nano plastics transport and sources.

HYSPLIT particle dispersion modelling was undertaken using the HYSPLIT concentration module and particle analysis, backwards modelling the trajectory using both wet and dry deposition for a conservative and illustrative release of 1 particle per hour for a 24 hr period, with cyclic emission repeated every 24 hours for the duration of the sample period. Particles were parameterised as: MP - 25 μm (the average MP particle size in the MP dataset), 1 g cc^{-1} (Kooi & Koelmans, 2019), settling velocity 0.02 m s^{-1}, default wet deposition of in and below cloud wet removal of 8.0E-05 s^{-1} (Draxler & Hess, G, 2018; Stein et al., 2015); NP - 0.45 μm, 1 g cc^{-1} (Kooi & Koelmans, 2019), settling velocity 6.3×10^{-6} m s^{-1}, cyclic emission of 1particle/hr for 24 hours repeated every 24 hours. The resulting particle plots were created to illustrate the extent of particle transport and the elevation (above ground level) relative to the monitoring period (Fig. 3). The atmospheric model was capped to 10,000 m a.g.l..

The model outputs identify MP to be transported generally at or below 2000 m a.g.l., with particles transport from relatively close to the site (<100 km, potentially due to resuspension of previously deposited atmospheric MP) to 10,000 km away. The spatial distribution for this high level visualisation of MP particle movement suggests particles to have been transported from and passing over Europe, north America, northern Africa and the Atlantic Ocean. Comparatively, NP particles appear to extend over a greater northern hemisphere spatial distance, extending down the north western (Atlantic) African coast, across China and the north Pacific Ocean and encroaching further into the Atlantic side of the Arctic circle than the modelled MP. NP particles occur through the modelled atmosphere, with notable particles predicted to occur above 2000 m a.g.l. compared to very few MP modelled at these higher elevations. NP in general were suggested to travel extended distance (<100 km) prior to occurring at the field site, with less occurrence of shorter travel compared to MPs.

The model results were disaggregated to try and identify the spatial 'source' areas for MP and NP to this field site using these very general particle parameters and gross sampling conditions. Modelled particle backward trajectories were followed to identify which particles would be found at 'ground level' (0-10 m a.g.l. adopted as the surface and entrainment zone), during the sample period (samples November to March 2018). All particles that fell to or below 10m a.g.l. were spatially plotted to identify indicative possible source locations for MP and NP for this site using this simple overview model.

High quantities of MP were found at or below 10m a.g.l. during the backward trajectory particle modelling, but notably fewer NP were found at this low elevation. The NP are noted to predominantly stay elevated over the modelled duration therefore presenting a lower particle count within the 0-10 m a.g.l. 'ground level' illustrated in Fig. 4. NP

Table 1
Potential source areas of MP and NP to this site for the monitored and modelled duration. Possible entrainment areas have been derived through comparison of HYSPLIT backward particle trajectory modelling (latitude, longitude and elevation to country spatial extent defined in the ESRI world country file WGS48 (Belgiu, 2015).

Microplastic						Nanoplastic		
Location	MP km^{-2}	Potential source*	Location	MP km^{-2}	Potential source*	Location	NP km^{-2}	Potential source*
Spain	0.00602	3%	Germany	0.000142	<1%	Norway	3.34E-06	1%
France	0.005094	3%	Kazakhstan	0.000136	<1%	Afghanistan	3.2E-06	1%
Norway	0.002261	1%	Montenegro	0.000132	<1%	United States	3.04E-06	15%
Andorra	0.001799	<1%	Belarus	8.52E-05	<1%	Kazakhstan	2.73E-06	4%
Canada	0.001395	24%	Mongolia	5.48E-05	<1%	Morocco	2.6E-06	<1%
Portugal	0.001379	<1%	Poland	5.38E-05	<1%	Canada	2.54E-06	18%
Croatia	0.001237	<1%	Kyrgyzstan	4.65E-05	<1%	Mauritania	2.22E-06	1%
Oceans and Seas	0.000120	43%	Hungary	4.53E-05	<1%	Uzbekistan	2.07E-06	<1%
Switzerland	0.000941	<1%	Macedonia	3.64E-05	<1%	Mali	1.88E-06	1%
Iceland	0.000879	<1%	Slovakia	3.35E-05	<1%	Algeria	1.87E-06	2%
Greenland	0.000851	6%	Czech Republic	3.05E-05	<1%	Sweden	1.27E-06	<1%
Finland	0.000806	1%	Belgium	2.57E-05	<1%	Turkey	1.23E-06	<1%
Netherlands	0.000684	<1%	Italy	2.42E-05	<1%	Russia	1.16E-06	15%
Romania	0.000615	<1%	Afghanistan	2.08E-05	<1%	Egypt	1.11E-06	<1%
Denmark	0.000537	<1%	Bulgaria	1.64E-05	<1%	Iran	6.4E-07	<1%
Russia	0.000522	15%	Algeria	1.5E-05	<1%	Greenland	6.05E-07	2%
Bosnia and Herzegovina	0.000414	<1%	Mauritania	1.33E-05	<1%	Saudi Arabia	5.75E-07	<1%
Faroe Islands	0.000393	<1%	Georgia	1.31E-05	<1%	Deomocratic Republic of the Congo	5.27E-07	<1%
Ireland	0.000385	<1%	Lithuania	1.09E-05	<1%	Sudan	4.79E-07	<1%
Estonia	0.00031	<1%	Austria	9.96E-06	<1%	Oceans and Seas	2.44E-07	38%
Moldova	0.0002	<1%	Western Sahara	8.33E-06	<1%	China	1.05E-07	<1%
United Kingdom	<1%	<1%	Tajikistan	6.8E-06	<1%			
Sweden	<1%	<1%	Uzbekistan	6.2E-06	<1%			
United States	<1%	2%	Ukraine	5.44E-06	<1%			
Serbia	<1%	<1%	Turkey	4.93E-06	<1%			
Latvia	<1%	<1%	China	3.47E-06	<1%			
Morocco	<1%	<1%	Mali	2.81E-06	<1%			

* % of total representative MP and NP particles derived from this location

remain elevated for an extended period of time compared to MP, and extend vertically across the entire troposphere (PBL and free troposphere) while MP altitudes are generally lower (<3000 m a.g.l.). Both MP and NP backward particle modelling suggests long distance transport, with particles falling close to ground level at distal locations relative to the monitoring location, alluding the sample plastic particles are not primarily locally sourced.

If the percentage of particles modelled at an elevation of ground level (≤10 m a.g.l.) are counted, the potential spatial source extents can be tentatively identified (Table 1) (for this sample period at this location). The backward particle modelling can identify possible source areas (through analysis of the location where particles are modelled to be at ground level), however, whether there is a plastic pollution source at the modelled location needs further detailed analysis.

Potential source areas were estimated from model outputs as MP or NP per km^2 and as a percentage of all particles ≤10 m a.g.l.. MP or NP per km^2 provide a spatially comparable surface 'emission' rate per designated area (country or ocean areas). The percentage values provide an indicative comparable land mass or ocean specific general contribution to the overall field site during this sample period. While it is acknowledged this is very indicative and not directly representative of the field samples, these results provide a first assessment of the potential gross source areas that may contribute MP and NP to this site.

The simplistic model assessment of potential MP and NP source areas suggests continental Europe (France, Spain, Andorra) and Norway to be key possible areas of MP when source is considered relative to area (MP km^{-2}). When considered as a proportion of the total modelled MP potentially transported to the field site during this monitored period, the marine environment (for example Atlantic Ocean, Mediterranean Ocean) are suggested to be significant contributors to atmospheric MP (43%).The Arctic Ocean also appears to be a contributor, conceding the marine Arctic plastic pollution as a possible source (Bergmann et al., 2022). NP appears to be transported from a greater distance, with Norway, south central Asia (Afghanistan), and north America suggested as possible areas of NP contribution. However, when considered by continent or ocean, the marine environment is suggested to a notable contributor to atmospheric NP at this site (38%), similar to MP model outputs (D. Allen et al., 2022; S. Allen et al., 2020). It is noted that a much greater number of NP particles would be expected for ≤10 m a.g.l. if the model was extended backward in time (if the backward particle trajectories were run for long enough to follow particle down to lower atmospheric elevations) rather than being constrained to the monitored duration of the field samples. However, for small NP this could be weeks or more and would change for each particle depending on its trajectory and environmental conditions, resulting in a highly complex and extensive dataset that is not considered appropriate for the overview transport modelling intended to support the MP and NP field findings in this study.

Conclusion

This study presents a direct comparison of NP and MP content in atmospheric deposition samples collected in a relatively remote area of the Pyrenees, France. While MP is analysed by particle and NP is analysed by mass, using simple volume to mass calculations a comparison has been made of both mass and particle count for MP and NP for this monitoring period. NP (<0.45 μm) were found to present a comparative mass compared to MP in the same sample, and a correspondingly much higher particle count (NP>>MP particles per sample). The MP and NP sample composition varies, with plastic polymer predominance in the MP particle size range not directly reflected in the NP proportion of the sample. This may be due to the atmospheric transport dynamics of

the different particle sizes, acknowledging the smaller NP particles fall within the realms of Brownian motion. The long distance transport necessary to create MP and NP at this sample location may also influence the sample composition, suggesting that NP may have been transported from more extensive distances from the site than MP particles. The HYSPLIT back trajectories illustrate the global long range atmospheric transport of nanoplastic and give indications of the possible source areas. Most notably the ocean is illustrated as the source of ~38% of global atmospheric emissions of nanoplastics. This finding suggests that whilst previous work has shown the ocean as a source for MP, it is also clearly the source of a much greater amount of nanoplastic, and as such requires urgent investigation.

Declaration of Competing Interest

The authors declare they have no competing interest.

CRediT authorship contribution statement

Steve Allen: Conceptualization, Resources, Methodology, Data curation, Investigation, Writing – original draft, Writing – review & editing. **Dušan Materić:** Conceptualization, Resources, Methodology, Data curation, Investigation, Writing – original draft, Writing – review & editing. **Deonie Allen:** Resources, Methodology, Data curation, Investigation, Writing – original draft, Writing – review & editing. **Anna MacDonald:** Data curation, Writing – original draft, Writing – review & editing. **Rupert Holzinger:** Resources, Writing – review & editing. **Gael Le Roux:** Resources, Writing – review & editing. **Vernon R Phoenix:** Resources, Writing – review & editing.

Acknowledgments

The authors would like to thank the Ocean Frontiers Institute (OFI) for the support of Steve Allen through the International Postdoctoral Fellowship, the Leverhulme Trust, grant ECF-2019-306, for their support of Deonie Allen and the EPSRC doctoral scholarship provided to Anna MacDonald (EP/T517938/1). The authors acknowledge the support provided to Gael Le Roux by the ANR-20-CE34-0014 Atmo-Plastic project, the Plasticopyr project within the Interreg V-A Spain-France- Andorra programme, the CNRS TRAM Project and ANR-15-CE01-0008, Observatoire Homme- Milieu Pyrénées Haut Vicdessos - LABEX DRIIHM ANR-11-LABX0010. The authors also acknowledge the support from Dutch Research Council (Nederlandse Organisatie voor Wetenschappelijk Onderzoek – NWO) projects: “Nanoplastics: hormone-mimicking and inflammatory responses?” (grant number OCENW.XS2.078) and “Size distribution of nanoplastics in indoor, urban and rural air” (grant number OCENW.XS21.2.042) provided to Dušan Materić.

Supplementary materials

Supplementary material associated with this article can be found, in the online version, at doi:10.1016/j.hazadv.2022.100104.

References

Akoueson, F., Chbib, C., Monchy, S., Paul-Pont, I., Doyen, P., Dehaut, A., Duflos, G., 2021. Identification and quantification of plastic additives using pyrolysis-GC/MS: a review. Sci. Total Environ. 773. doi:10.1016/j.scitotenv.2021.145073.

Allen, D., Allen, S., Jickells, T., Abbasi, S., Baker, A., Bergmann, M., Brahney, J., Butler, T., Dusan, M., Eckhart, S., Kanakidou, M., Laj, P., Levermore, J., Li, D., Liss, P., Liu, K., Majowald, N., Masque, P., Mayes, A., … Duce, R., 2022. The atmospheric cycle of microplastics in the marine environment. Nat. Rev. Earth Environ. doi:10.1038/s43017-022-00292-x.

Allen, S., Allen, D., Moss, K., Le Roux, G., Phoenix, V.R., Sonke, J., 2020. Examination of the ocean as a source for atmospheric microplastics. PLoS One 15 (5), e0232746. doi:10.1371/journal.pone.0232746.

Allen, S., Allen, D., Phoenix, V.R., Le Roux, G., Duranteza, P., Simonneau, A., Stéphane, B., Galop, D., 2019. Atmospheric transport and deposition of microplastics in a remote mountain catchment. Nat. Geosci. 12, 339–344. doi:10.1038/s41561-019-0335-5.

Ambrosini, R., Azzoni, R.S., Pittino, F., Diolaiuti, G., Franzetti, A., Parolini, M., 2019. First evidence of microplastic contamination in the supraglacial debris of an alpine glacier. Environ. Pollut. 253, 297–301. doi:10.1016/j.envpol.2019.07.005.

Banerjee, A., Shelver, W.L., 2021. Micro- and nanoplastic induced cellular toxicity in mammals: A review. Sci. Total Environ. 755, 142518. doi:10.1016/j.scitotenv.2020.142518.

Belgiu, M., 2015. UIA Latitude/Longitude Graticules and World Countries Boundaries. ArcGIS Hub.

Bergmann, M., Collard, F., Fabres, J., Gabrielsen, G.W., Provencher, J.F., Rochman, C.M., van Sebille, E., Tekman, M.B., 2022. Plastic pollution in the Arctic. Nat. Rev. Earth Environ. 3 (May), 323–337. doi:10.1038/s43017-022-00279-8.

Bergmann, M., Mützel, S., Primpke, S., Tekman, M.B., Trachsel, J., Gerdts, G., 2019. White and wonderful? Microplastics prevail in snow from the Alps to the Arctic. Sci. Adv. 5 (8), eaax1157. doi:10.1126/sciadv.aax1157.

Bianco, A., Passananti, M., 2020. Atmospheric Micro and Nanoplastics : An Enormous Microscopic Problem. Sustainability 12, 7327. doi:10.3390/su12187327.

Cabrera, M., Valencia, B.G., Lucas-Solis, O., Calero, J.L., Maisincho, L., Conicelli, B., Massaine Moulatlet, G., Capparelli, M.V., 2020. A new method for microplastic sampling and isolation in mountain glaciers: A case study of one antisana glacier, Ecuadorian Andes. Case Stud. Chem. Environ. Eng. 2 (September), 100051. doi:10.1016/j.cscee.2020.100051.

Deng, Y., Yan, Z., Shen, R., Wang, M., Huang, Y., Ren, H., Zhang, Y., Lemos, B., 2020. Microplastics release phthalate esters and cause aggravated adverse effects in the mouse gut. Environ. Int. 143, 105916. doi:10.1016/j.envint.2020.105916.

Draxler, R.R., Hess, G, D, 2018. Description of the Hysplit4 modeling system.

Ferreira, I., Venâncio, C., Lopes, I., Oliveira, M., 2019. Nanoplastics and marine organisms: What has been studied? Environ. Toxicol. Pharmacol. 67 (November 2018), 1–7. doi:10.1016/j.etap.2019.01.006.

Feynman, R., 1963. Brownian motion. Feynman Lectures.

Frias, J.P.G.L., Nash, R., 2019. Microplastics: Finding a consensus on the definition. Mar. Pollut. Bull. 138 (November 2018), 145–147. doi:10.1016/j.marpolbul.2018.11.022.

Gigault, J., El Hadri, H., Nguyen, B., Grassl, B., Rowenczyk, L., Tufenkji, N., Feng, S., Wiesner, M., 2021. Nanoplastics are neither microplastics nor engineered nanoparticles. Nat. Nanotechnol. 16 (5), 501–507. doi:10.1038/s41565-021-00886-4.

Gonçalves, J.M., Bebianno, M.J., 2021. Nanoplastics impact on marine biota: A review. Environ. Pollut. 273. doi:10.1016/j.envpol.2021.116426.

Huang, J.N., Wen, B., Zhu, J.G., Zhang, Y.S., Gao, J.Z., Chen, Z.Z., 2020. Exposure to microplastics impairs digestive performance, stimulates immune response and induces microbiota dysbiosis in the gut of juvenile guppy (Poecilia reticulata). Sci. Total Environ. 733, 138929. doi:10.1016/j.scitotenv.2020.138929.

Joachim, C., 2005. To be nano or not to be nano? Nat. Mater. 4 (2), 107–109. doi:10.1038/nmat1319.

Kelly, A., Lannuzel, D., Rodemann, T., Meiners, K.M., Auman, H.J., 2020. Microplastic contamination in east Antarctic sea ice. Mar. Pollut. Bull. 154 (January), 111130. doi:10.1016/j.marpolbul.2020.111130.

Kooi, M., Koelmans, A.A., 2019. Simplifying microplastic via continuous probability distributions for size, shape, and density. Environ. Sci. Technol. Lett. 6 (9), 551–557. doi:10.1021/acs.estlett.9b00379.

Li, B., Ding, Y., Cheng, X., Sheng, D., Xu, Z., Rong, Q., Wu, Y., Zhao, H., Ji, X., Zhang, Y., 2020. Polyethylene microplastics affect the distribution of gut microbiota and inflammation development in mice. Chemosphere 244, 125492. doi:10.1016/j.chemosphere.2019.125492.

Li, T., Raizen, M.G., 2013. Brownian motion at short time scales. Ann. Phys. 525 (4), 281–295. doi:10.1002/andp.201200232.

Materić, D., Kasper-Giebl, A., Kau, D., Anten, M., Greilinger, M., Ludewig, E., van Sebille, E., Röckmann, T., Holzinger, R., 2020. Micro- and nanoplastics in Alpine snow – a new method for chemical identification and quantification in the nanogram range. Environ. Sci. Technol. 54 (5), 2353–2359. doi:10.1021/acs.est.9b07540.

Materić, D., Kjær, H.A., Vallelonga, P., Tison, J.-L., Rockmann, T., Holzinger, R., 2022. Nanoplastics measurements in Northern and Southern polar ice. Environ. Res. 208, 112741. doi:10.1016/j.envres.2022.112741.

Materić, D., Ludewig, E., Brunner, D., Rochmann, T., Holzinger, R., 2021. Nanoplastics transport to the remote, high-altitude Alps. Environ. Pollut. (117697) 288. doi:10.1016/j.envpol.2021.117697.

Menges, F., 2018. *Spectragryph* (v1.2.8).

Mitrano, D.M., Wick, P., Nowack, B., 2021. Placing nanoplastics in the context of global plastic pollution. Nat. Nanotechnol. 1–10. doi:10.1038/s41565-021-00888-2.

Munno, K., Frond, H.De, Donnell, B.O., Rochman, C.M, 2020. Increasing the accessibility for characterizing microplastics : Introducing new application-based and spectral libraries of plastic particles (SLoPP & SLoPP-E). Anal. Chem. 92 (3), 2443–2451. doi:10.1021/acs.analchem.9b03626.

Okoffo, E.D., Ribeiro, F., O'Brien, J.W., O'Brien, S., Tscharke, B.J., Gallen, M., Samanipour, S., Mueller, J.F., Thomas, K.V., 2020. Identification and quantification of selected plastics in biosolids by pressurized liquid extraction combined with double-shot pyrolysis gas chromatography–mass spectrometry. Sci. Total Environ. 715 (January), 136924. doi:10.1016/j.scitotenv.2020.136924.

Piccardo, M., Renzi, M., Terlizzi, A., 2020. Nanoplastics in the oceans: theory, experimental evidence and real world. Mar. Pollut. Bull. 157 (April), 111317. doi:10.1016/j.marpolbul.2020.111317.

Plastics Europe, & Organisations, E. A. O. P. R. & R, 2021. Plastics - the Facts 2021.

Primpke, S., Cross, R.K., Mintenig, S., Simon, M., Vianello, A., Gerdts, G., Vollertsen, J., 2020. Toward the Systematic Identification of Microplastics in the Environment: Evaluation of a New Independent Software Tool (siMPle) for Spectroscopic Analysis. Appl. Spectrosc. 74 (9), 1127–1138. doi:10.1177/0003702820917760.

Rubio, L., Marcos, R., Hernández, A., 2020. Potential adverse health effects of ingested micro- and nanoplastics on humans. Lessons learned from in vivo and in

vitro mammalian models. J. Toxicol. Environ. Health - Part B 23 (2), 51–68. doi:10.1080/10937404.2019.1700598.

Stein, A.F., Draxler, R.R., Rolph, G.D., Stunder, B.J.B., Cohen, M.D., Ngan, F., Dohen, M., Ngqn, F., 2015. NOAA's HYSPLIT Atmospheric Transport and Dispersion Modeling System. Bull. Am. Meteorol. Soc. 96 (12), 2059–2077. doi:10.1175/BAMS-D-14-00110.1.

Trainic, M., Flores, J.M., Pinkas, I., Pedrotti, M.L., Lombard, F., Bourdin, G., Gorsky, G., Boss, E., Rudich, Y., Vardi, A., Koren, I., 2020. Airborne microplastic particles detected in the remote marine atmosphere. Commun. Earth Environ. 1 (1), 1–9. doi:10.1038/s43247-020-00061-y.

Wahl, A., Le Juge, C., Davranche, M., El Hadri, H., Grassl, B., Reynaud, S., Gigault, J., 2021. Nanoplastic occurrence in a soil amended with plastic debris. Chemosphere 262. doi:10.1016/j.chemosphere.2020.127784.

Wright, S. L., & Kelly, F. J. (2017). Plastic and human health: a micro issue?*Environ. Sci. Technol.*, 51(12), 6634–6647. https://doi.org/10.1021/acs.est.7b00423.

Wright, S.L., Ulke, J., Font, A., Chan, K.L., Kelly, F.J., 2020. Atmospheric microplastic deposition in an urban environment and an evaluation of transport. Environ. Int. 136, 105411. doi:10.1016/j.envint.2019.105411.

Xu, J.L., Thomas, K.V., Luo, Z., Gowen, A.A., 2019. FTIR and Raman imaging for microplastics analysis: State of the art, challenges and prospects. TrAC - Trends Anal. Chem. 119, 115629. doi:10.1016/j.trac.2019.115629.

Yang, T., Luo, J., Nowack, B., 2021. Characterization of Nanoplastics, Fibrils, and Microplastics Released during Washing and Abrasion of Polyester Textiles. Environ. Sci. Technol. 55 (23), 15873–15881. doi:10.1021/acs.est.1c04826.

Yee, M.S.L., Hii, L.W., Looi, C.K., Lim, W.M., Wong, S.F., Kok, Y.Y., Tan, B.K., Wong, C.Y., Leong, C.O., 2021. Impact of microplastics and nanoplastics on human health. Nanomaterials 11 (2), 1–23. doi:10.3390/nano11020496.

Zheng, Y., Li, J., Sun, C., Cao, W., Wang, M., Jiang, F., Ju, P., 2021. Comparative study of three sampling methods for microplastics analysis in seawater. Sci. Total Environ. 765, 144495. doi:10.1016/j.scitotenv.2020.144495.